

11-10-2009

g Factor of the 2^+_1 State of ^{172}Hf

Z. Berant

E. Oster

R. J. Casperson

A. Wolf

V. Werner

*See next page for additional authors*Follow this and additional works at: <http://scholarship.richmond.edu/physics-faculty-publications>Part of the [Nuclear Commons](#)

Recommended Citation

Berant, Z., E. Oster, R. J. Casperson, A. Wolf, V. Werner, A. Heinz, R. F. Casten, G. Gurdal, E. A. Mccutchan, D. S. Brenner, J. R. Terry, R. Winkler, E. Williams, J. Qian, A. Schmidt, M. K. Smith, T. Ahn, C. W. Beausang, P. H. Regan, T. Ross, M. Bunce, B. Darakchieva, D. A. Meyer, J. Leblanc, K. Dudziak, C. Bauer, and G. Henning. "g Factor of the 2^+_1 State of ^{172}Hf ." *Physical Review C* 80, no. 5 (November 10, 2009): 057303: 1 - 057303: 4. doi:10.1103/PhysRevC.80.057303.

This Article is brought to you for free and open access by the Physics at UR Scholarship Repository. It has been accepted for inclusion in Physics Faculty Publications by an authorized administrator of UR Scholarship Repository. For more information, please contact scholarshiprepository@richmond.edu.

Authors

Z. Berant, E. Oster, R. J. Casperson, A. Wolf, V. Werner, A. Heinz, R. F. Casten, G. Gurdal, E. A. McCutchan, D. S. Brenner, J. R. Terry, R. Winkler, E. Williams, J. Qian, A. Schmidt, M. K. Smith, T. Ahn, C. W. Beausang, P. H. Regan, T. J. Ross, M. Bunce, B. Darakchieva, D. A. Meyer, J. LeBlanc, K. Dudziak, C. Bauer, and G. Henning

g factor of the 2_1^+ state of ^{172}Hf

Z. Berant,^{1,2} E. Oster,² R. J. Casperson,¹ A. Wolf,^{1,2} V. Werner,¹ A. Heinz,¹ R. F. Casten,¹ G. Gurdal,³ E. A. McCutchan,⁴ D. S. Brenner,^{1,5} J. R. Terry,¹ R. Winkler,¹ E. Williams,¹ J. Qian,¹ A. Schmidt,¹ M. K. Smith,¹ T. Ahn,¹ C. W. Beausang,⁶ P. H. Regan,⁷ T. Ross,^{6,7} M. Bunce,^{1,7} B. Darakchieva,⁸ D. A. Meyer,⁸ J. LeBlanc,⁸ K. Dudziak,⁸ C. Bauer,⁹ and G. Henning^{1,10}

¹Wright Nuclear Structure Laboratory, Yale University, New Haven, Connecticut 06520, USA

²Nuclear Research Center Negev, Beer-Sheva 84190, Israel

³Rutgers University, New Brunswick, New Jersey 08903, USA

⁴Physics Division, Argonne National Laboratory, Argonne, Illinois 60439, USA

⁵Chemistry Department, Clark University, Worcester, Massachusetts 01610, USA

⁶Physics Department, University of Richmond, Richmond, Virginia 23173, USA

⁷Department of Physics, University of Surrey, Guildford, GU2 7XH, United Kingdom

⁸Rhodes College, Department of Physics, Memphis, Tennessee 38112, USA

⁹Institut für Kernphysik, Technische Universität Darmstadt, Darmstadt D-64289, Germany

¹⁰ENS CACHAN, France

(Received 17 August 2009; published 10 November 2009)

The g factor of the 2_1^+ state of ^{172}Hf was measured using the perturbed angular correlation technique in a static external magnetic field. The result, $g(2_1^+) = 0.25(5)$, is discussed in relation to the systematics of the previously reported g factors in the Hf isotopes and compared with the predictions of several models. An interesting outcome of the analysis presented in this paper is the agreement between the calculated g factors within the interacting boson approximation (IBA) and the results of a large-scale shell model calculation. This agreement supports the emphasis in the IBA on the valence space. The undershooting of the empirical g factors near midshell in both models suggests that they underestimate the role of the saturation of collectivity, which is explicitly incorporated into a phenomenological model that agrees better with the data.

DOI: [10.1103/PhysRevC.80.057303](https://doi.org/10.1103/PhysRevC.80.057303)

PACS number(s): 21.10.Ky, 23.20.En, 27.70.+q

A series of measurements of g factors of 2_1^+ states in proton-rich nuclei in the $A = 160$ region has recently been undertaken at the Wright Nuclear Structure Laboratory (WNSL) at Yale University. Experimental results have been obtained for Er, Yb, and Hf isotopes [1–3]. An interesting trend, previously established only for the Pt isotopes [4], has been observed also for the Yb and Hf isotopic chains. The main feature is that g factors in these isotopic chains have a very weak dependence on neutron number in the range from $N = 96$ to $N = 108$, weaker than the predictions of the hydrodynamical model [5]. These experimental observations have triggered several theoretical studies [6,7] that have attempted to explain the results—either using a phenomenological approach [6] or via large-scale shell model microscopic calculations [7]. The continuation of this series of experiments is therefore of particular interest to better establish the experimental observations and their theoretical implications for the understanding of nuclear structure in this region.

In this Brief Report, we present the results of a measurement of the g factor of the $I^\pi = 2_1^+$ state in ^{172}Hf . The half-life of this state was recently remeasured at WNSL [8] and found to be 1.278(40) ns. Since this is a relatively long half-life, we used the integral perturbed angular correlation method. The experimental technique and setup were described in some detail in Ref. [1]. The parent of ^{172}Hf , ^{172}Ta , was produced by the reaction $^{165}\text{Ho}(^{12}\text{C}, 5n)^{172}\text{Ta}$, with a 17 pA, 84 MeV ^{12}C beam from the tandem accelerator at WNSL. The ^{172}Ta nuclei were deposited on an aluminized tape collector and periodically transported to the center of a superconducting coil

capable of producing magnetic fields of up to 6 T. The half-life of ^{172}Ta is ~ 37 min, and the cycle of source accumulation-transport-counting was chosen to be 80 min. Eight high-purity germanium detectors, with relative efficiencies of 20–25%, were placed around the superconducting coil, at about 11 cm from its center; these detectors were used to measure the decay of the ^{172}Ta source to excited states in the daughter ^{172}Hf . Two runs were carried out, with two different magnetic field settings: 3.80 and 5.55 T. The magnetic fields were determined using the field vs current calibration function supplied by the manufacturer of the superconducting coil and checked using a calibrated Hall probe. The running time was approximately 160 h for each field direction, so the total running time for both field directions and both values of the magnetic field was about 640 h. About 5×10^8 γ - γ coincidence events were recorded and analyzed off-line. In the sorting procedure, all events originating from pairs of detectors with the same angular separation were sorted in the same spectrum. Special care was taken to ensure that the convention [9] of the signs of angles were observed. In Fig. 1, we present an example of a total projection γ - γ coincidence matrix.

To determine the g factor, we used the double ratio

$$R(\theta, B) = \left[\frac{I(\theta, B)}{I(\theta, -B)} \right] / \left[\frac{I(-\theta, B)}{I(-\theta, -B)} \right]^{1/2}, \quad (1)$$

where $I(\theta, B)$ is the coincidence intensity at angle θ and external field B . The use of this relation has the advantage that it eliminates the need of normalization for total integrated current on the target for field up and field down, and the

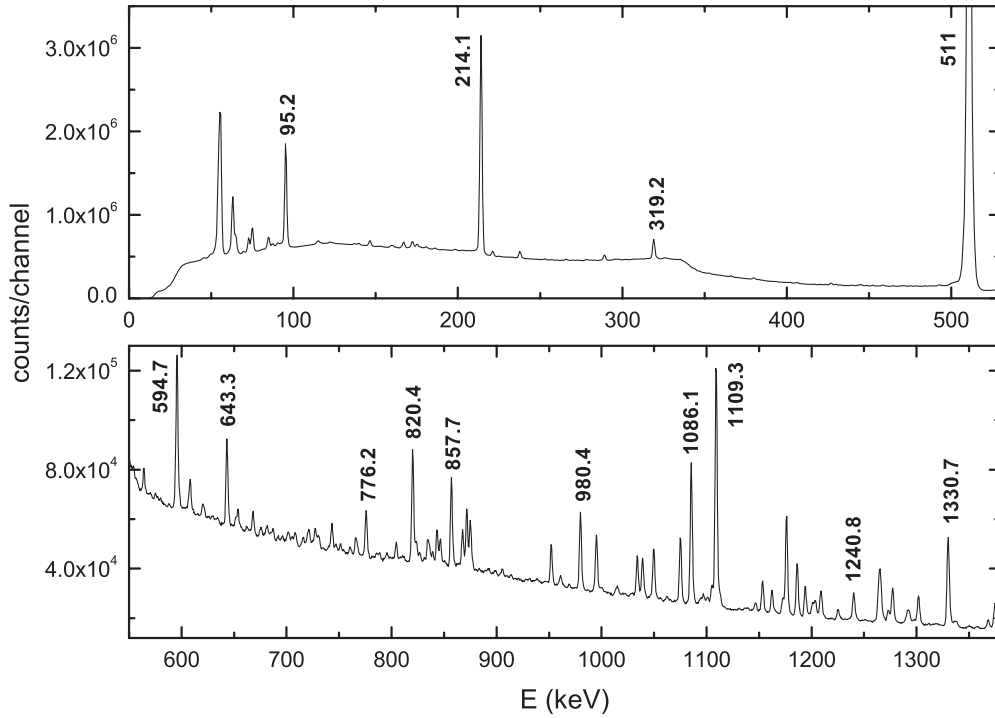


FIG. 1. Total projection of a γ - γ coincidence matrix obtained in the current work. All lines labeled by their energy in keV are observed following the β decay of ^{172}Ta to ^{172}Hf .

different relative efficiencies of detector pairs cancel out and need not be accounted for. The coincidence intensity $I(\theta, B)$ for a given spin sequence can be calculated using the formalism given by Frauenfelder and Steffen [10]. Of all the relevant γ - γ cascades, the maximum perturbation effect is obtained at detector angles of 145° and 35° for $0^+ \rightarrow 2^+ \rightarrow 0^+$ spin cascades. We therefore used the double ratio for the 776–95 keV, $0_2^+ \rightarrow 2_1^+ \rightarrow 0_1^+$ cascade to extract the g factor of the 2_1^+ state of ^{172}Hf from the data. The eight germanium detectors were set in such a way that 12 pairs were at $145^\circ(35^\circ)$, eight pairs were at $110^\circ(70^\circ)$, four pairs were at $105^\circ(75^\circ)$, and the remaining four pairs were at 180° . This setup maximizes the statistics at 145° and 35° . In addition to the 776–95 keV transition, the double ratio $R(\theta, B)$ was also calculated for five other cascades: 214–95, 858–95, 980–95, 1086–95, and 1241–95 keV. The values of the double ratio calculated from the data for all six cascades considered in this experiment are given in Table I. We also extracted the double ratios at 180° from the data. At this angle, the double ratio should be 1.00 for all cascades, so the experimental results can be used to check for systematic errors. To determine the g factor, we calculated the functions $R(145^\circ, B)$ vs g for a $0^+ \rightarrow 2^+ \rightarrow 0^+$ cascade for $B = 3.80$ and 5.55 T. These two functions are presented in Fig. 2. Comparison of the functions in Fig. 2 with the experimental results given in Table I for the 776–95 keV cascade for both values of the magnetic field yields two values of the g factor:

$$g(2_1^+)_{\text{exp}}^{3.80\text{T}} = 0.23(6), \quad (2)$$

$$g(2_1^+)_{\text{exp}}^{5.55\text{T}} = 0.28(8). \quad (3)$$

The weighted mean of these two values gives the final experimental value of this work:

$$g(2_1^+)_{\text{exp}} = 0.25(5). \quad (4)$$

The result for the 1241–95 keV cascade was initially intended to be used to improve the error bar of the experimental g factor, since the level at 1336 keV was believed to be a 0_4^+ state [11]. However, comparison of the result of the double

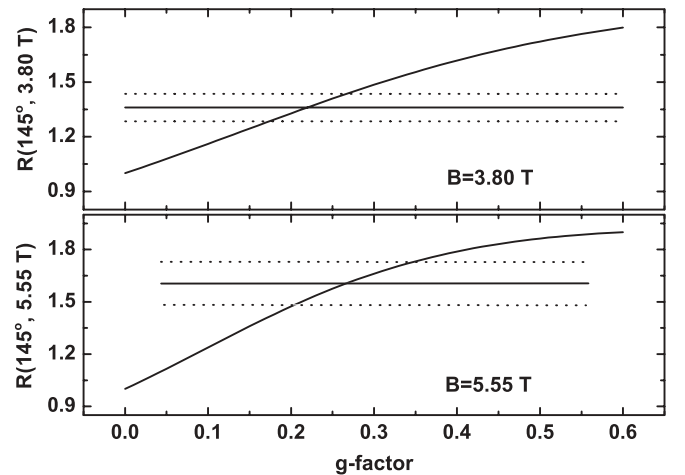


FIG. 2. Calculated double ratio $R(145^\circ, B)$ vs the g factor, and the experimental double ratio for the 776–95 keV cascade, for the two values of the magnetic field used in this experiment. The solid and dotted horizontal lines indicate the experimental values and their errors.

TABLE I. Values of the double ratio $R(\theta, B)$ obtained from the coincidence data for several cascades of ^{172}Hf .

Cascade (keV)	Spin sequence	Angle (deg)	$R_{\text{exp}}(\theta, 3.80 \text{ T})$	$R_{\text{exp}}(\theta, 5.55 \text{ T})$	$R_{\text{calc}}(\theta, 3.80 \text{ T})^a$	$R_{\text{calc}}(\theta, 5.55 \text{ T})^a$
776–95	$0_2^+ - 2_1^+ - 0_1^+$	145	1.36(8)	1.61(12)	–	–
1241–95	$(0)_4^+ - 2_1^+ - 0_1^+$	145	0.87(8)	0.98(7)	–	–
214–95	$4_1^+ - 2_1^+ - 0_1^+$	145	1.031(6)	1.017(7)	1.02(1)	1.03(1)
858–95	$2_2^+ - 2_1^+ - 0_1^+$	145	1.17(5)	1.22(6)	1.07(1) ^b	1.09(1) ^b
980–95	$2_3^+ - 2_1^+ - 0_1^+$	145	1.10(5)	1.09(5)	1.07(1) ^b	1.09(1) ^b
1086–95	$3_1^+ - 2_1^+ - 0_1^+$	145	0.97(3)	0.97(3)	0.93(1) ^b	0.90(1) ^b
776–95	$0_2^+ - 2_1^+ - 0_1^+$	180	1.08(7)	1.07(7)	1.00	1.00
1241–95	$(0)_4^+ - 2_1^+ - 0_1^+$	180	1.14(16)	–	1.00	1.00
214–95	$4_1^+ - 2_1^+ - 0_1^+$	180	1.021(8)	1.019(10)	1.00	1.00
857–95	$2_2^+ - 2_1^+ - 0_1^+$	180	1.08(7)	1.07(7)	1.00	1.00
980–95	$2_3^+ - 2_1^+ - 0_1^+$	180	1.04(8)	0.95(9)	1.00	1.00
1086–95	$3_1^+ - 2_1^+ - 0_1^+$	180	1.00(5)	1.01(11)	1.00	1.00

^aValues of R_{calc} and its error bars, where given, were obtained using the value $g(2_1^+)_{\text{exp}} = 0.25(5)$ (see text).

^bThe double ratio was calculated assuming pure $E2$ character for the first transition of the cascade.

ratio for this cascade, given in Table I, with that of the 776–95 keV cascade, shows clearly that this assignment is wrong. The results for the remaining four cascades in Table I are used as a consistency check. In the sixth and seventh columns of the table, we present the values of the double ratios for these cascades, calculated using the g factor in Eq. (4). We note that the double ratio at 180° is expected to be 1.00 for all spin sequences. The agreement between the calculated and experimental values in Table I indicates that systematic errors, if present, are within the statistical errors of the experiment.

We now discuss the experimental values obtained in this experiment in the framework of several models and theoretical calculations: the two versions (rotational and vibrational) of the hydrodynamical model [5], the proton-neutron version of the interacting boson approximation (IBA-2) [12], the phenomenological model of Jing-ye *et al.* [6], and the recently reported large-scale shell model calculation of Bao-An Bin *et al.* [7]. The experimental result of the present experiment, the recently reported result for ^{170}Hf [3], and the results for $^{176,178,180}\text{Hf}$ from the compilation of Stone [13] are presented in Fig. 3, together with the predictions of the models and calculations mentioned above. For the proton-neutron version of the interacting boson approximation, we used the relation [12]

$$g(2_1^+) = \frac{g_\pi N_\pi + g_\nu N_\nu}{N_\pi + N_\nu}, \quad (5)$$

where N_π and N_ν are the number of valence proton and neutron bosons, and g_π , g_ν are the boson g factors. For the latter parameters, we used the values $g_\pi = 0.63$ and $g_\nu = 0.05$ [14]. From Fig. 3, we see that the present result follows the trend observed previously [3], namely, that the g factors of the Hf isotopes are almost constant in the range $N = 98$ –108. Although the error bars are too large to allow an unambiguous differentiation between the models and calculations presented in Fig. 3, the phenomenological model of Zhang *et al.* [6] seems to give the best overall description of the data. This model uses the concept of effective boson numbers [14] and assumes a reduction of the effective numbers of protons and neutrons across midshell. The results presented in this Brief

Report, together with the previously reported data, confirm the validity of the concept of effective boson numbers. In Fig. 3, we also present the effective neutron boson numbers N_{veff} together with the normal neutron boson numbers N_ν . We clearly see the saturation effect of the effective boson number, which is responsible for the experimentally observed constant values of the g factors vs N and also for the well-known saturation of the $B(E2)$ value in the same region [6].

Another interesting feature of Fig. 3, which is also found for other nearby isotopic chains, is the good agreement between

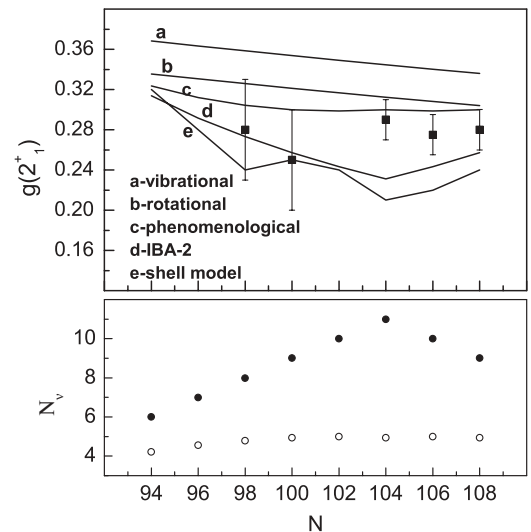


FIG. 3. Systematics of $g(2_1^+)$ data for the Hf isotopes. The result for $N = 98$ is from our previous measurement [3], the value at $N = 100$ is from this experiment, and the other three experimental points are from Stone's tabulation in Ref. [13]. The data are compared with the predictions of several models: the rotational and vibrational limits of the hydrodynamical model [5], the IBA-2 [12], the phenomenological model of Zhang *et al.* [6], and the results of a large-scale shell model microscopic calculation [7]. The number of neutron bosons N_ν (black circles) and the number of neutron effective bosons (open circles), calculated with the phenomenological model [6], are also shown.

the large-scale shell model calculation [7] and the predictions of the interacting boson approximation in the mass range $A = 150\text{--}200$. We note, however, that the IBA-2 predictions were obtained using the analytical formula given above, which is valid only for the three limiting symmetries of this model. To better establish the comparison with the large-scale shell model calculation, we performed several numerical IBA-2 calculations of the g factors in Fig. 3, using the code NPBOS [15] and parameters that were chosen following published theoretical works for nuclei in this region [15,16]. The results confirmed the trend as well as the absolute values predicted by the analytical formula [Eq. (5)]. The similarity between the IBA-2 results and those from the large-scale shell model calculations suggests that the IBA-2 captures essential physics embodied in its focus on the valence space and in the different contributions of protons and neutrons. The fact that both calculations underestimate the data near

midshell, compared to the phenomenological model, suggests that they underestimate the saturation aspects of nuclear collectivity in regions with large numbers of valence nucleons. Further measurements of g factors in this region are under way, and it is expected they will trigger more theoretical investigations.

The authors are indebted to the staff of the Wright Nuclear Structure Laboratory for the skillful operation of the tandem accelerator and especially to Mr. Walter R. Garnett, Jr., for extensive technical support. A.W. and P.H.R. acknowledge the hospitality of the WNSL during the experiment. This work was supported by the US DOE under Grant Nos. DE-FG02-91ER-40609, DE-AC02-06CH11357, and DE-FG02-88ER-40417; the US NSF under Grant No. PHY-0245018; the Yale Flint Fund; and the STFC(UK) and YUUP under Project No. DPT2006K-120470.

-
- [1] Z. Berant *et al.*, Phys. Rev. C **69**, 034320 (2004).
 [2] A. Wolf *et al.*, Phys. Rev. C **72**, 027301 (2005).
 [3] A. Wolf *et al.*, Phys. Rev. C **76**, 047308 (2007).
 [4] A. E. Stuchbery *et al.*, Phys. Rev. Lett. **76**, 2246 (1996).
 [5] W. Greiner, Nucl. Phys. **80**, 417 (1966).
 [6] Jing-ye Zhang *et al.*, Phys. Rev. C **73**, 037301 (2006).
 [7] Bao-An Bian, Yao-Min Di, Gui-Lu Long, Yang Sun, Jing-ye Zhang, and Javid A. Sheikh, Phys. Rev. C **75**, 014312 (2007).
 [8] M. R. Bunce, M.Sc. thesis, University of Surrey, 2009.
 [9] O. Dørum and B. Selsmark, Nucl. Instrum. Methods **97**, 243 (1971).
 [10] H. Frauenfelder and R. M. Steffen, in *Alpha-, Beta-, and Gamma-Ray Spectroscopy*, edited by K. Siegbahn (North-Holland, Amsterdam, 1965), p. 1151.
 [11] *Table of Isotopes*, 8th ed., edited by R. Firestone and V. Shirley (Wiley, New York, 1996).
 [12] M. Sambataro, O. Scholten, A. E. L. Dieperink, and G. Piccitto, Nucl. Phys. **A423**, 333 (1984).
 [13] N. J. Stone, Table of Nuclear Magnetic Dipole and Electric Quadrupole Moments, NNDC, 2001 (unpublished), <http://www.nndc.bnl.gov/publications/preprints/nuclear-moments.pdf>.
 [14] A. Wolf and R. F. Casten, Phys. Rev. C **36**, 851 (1987).
 [15] G. Puddu, O. Scholten, and T. Otsuka, Nucl. Phys. **A348**, 109 (1980).
 [16] R. Bijker, A. E. L. Dieperink, O. Scholten, and R. Spanhoff, Nucl. Phys. **A344**, 207 (1980).